

## 졸-겔 반응을 통한 폴리비닐피롤리돈을 이용한 실리카 코팅된 흑연의 제조

남정훈 · 김영선 · 김경희 · 백성현 · 박동화 · 심상은<sup>†</sup>

인하대학교 화학·화학공학 융합대학원

(2015년 8월 28일 접수, 2015년 9월 24일 수정, 2015년 9월 25일 채택)

### Synthesis of Alumina-coated Graphite Using Polyvinylpyrrolidone via Sol-Gel Reaction

Jeonghoon Nam, Yeongseon Kim, and Kyunghee Kim, Sung Hyeon Baek,  
Dong Wha Park, and Sang Eun Shim<sup>†</sup>

Department of Chemistry & Chemical Engineering, Inha University, 253 Yonghyundong, Namgu, Incheon 22212, Korea

(Received August 28, 2015; Revised September 24, 2015; Accepted September 25, 2015)

**초록:** 흑연은 200~800 W/mK의 우수한 열전도성을 지니고 있으나, 인쇄회로기판의 코팅 재료, 반도체 실장용 접착제의 충전제, 열확산 슈트와 같은 열전도성 복합재료로 사용하기에 한계가 있다. 이는 전기 전도성에 기인한 것으로, 흑연에 전기 절연성을 부여하기 위하여 폴리비닐피롤리돈(PVP)을 접착력 향상제로 사용하여 알루미늄 층을 코팅하였다. 알루미늄 이소프로폭사이드(AIP)를 알루미늄의 전구체로 사용하였다. 알루미늄 코팅은 염기성 촉매하에서 졸-겔 반응을 통하여 이루어졌다. 제조된 결과물의 모폴로지 변화, 코팅된 알루미늄의 양 및 전기 절연성이 조사되었으며, 최적의 알루미늄@PVP@흑연의 합성 조건을 찾기 위하여 AIP와 PVP의 양을 변화시켰다. 합성된 알루미늄이 코팅된 흑연은 면저항이 1012 ohm/sq으로 전기 절연성을 보유했다.

**Abstract:** Although graphite has excellent thermal conductivity of 200-800 W/mK, there are definite limits when applying graphite to thermally conductive materials, such as a coating material for printed circuit boards (PCB), an additive to the adhesive for the assembly of electronic chips, and a filler for thermal spreader pads. The problems are largely attributed to the electrically conductive property. To endow graphite with an electrically insulating property, graphite was coated with a well-grown alumina layer using polyvinylpyrrolidone (PVP) as a cohesive promotor. Aluminum isopropoxide (AIP) was used as the alumina precursor and PVP was used to improve the cohesion between graphite and alumina. An alumina-coating on graphite was conducted by a base-catalyzed sol-gel reaction. The changes in the morphology and the amounts of coated alumina, as well as the electrically insulating properties were investigated. An optimized condition to make alumina@PVP@graphite was determined by changing the amounts of AIP and PVP. The synthesized alumina@PVP@graphite was categorized as an electrical insulator with a high surface resistivity of about  $10^{12}$  ohm/sq.

**Keywords:** alumina coating, graphite, sol-gel reaction.

## Introduction

The importance of the thermal management of electronic devices has been highlighted with the demands in the fields of electronic devices, which have become more compact and lighter. The transistor dimensions of computer chips have decreased and the power densities have increased. The clock

speeds have also risen exponentially. These changes make these electronic devices more prone to malfunctions and destruction at high temperature. Therefore, a method to remove heat from the electronic devices in a short time helps improve the life-time and the efficiency of operation.<sup>1-5</sup> For these reasons, thermally conductive fillers have been used to fabricate thermally conductive materials, such as printed circuit boards (PCB), heat sinks, housings, integrated heat spreaders, under-fill materials, thermal adhesives, and the applications of thermal interfacial materials. Carbonaceous filler, such as graphite, graphene, and carbon nanotubes (CNTs), and ceramic fillers

<sup>†</sup>To whom correspondence should be addressed.

E-mail: seshim@inha.ac.kr

©2016 The Polymer Society of Korea. All rights reserved.

**Table 1. Reaction Conditions for Alumina Coating on the Surface of the Graphite according to Various Contents of AIP**

No.	Precursor (wt% to graphite)	Graphite KS6 + KS44 (G, 1:1 wt%)	NH <sub>4</sub> OH (mL)	EtOH (mL)	PVP (g)
1	20				
2	40				
3	60				
4	80	2	2	50	3.2
5	120				
6	160				

**Table 2. Reaction Conditions for Alumina Coating on the Surface of the Graphite according to Various Contents of PVP**

No.	PVP (wt% to graphite)	Graphite KS6 + KS44 (G, 1:1 wt%)	NH <sub>4</sub> OH (mL)	EtOH (mL)	Precursor (g)
1	0				
2	20				
3	40	2	2	50	2.4
4	80				
5	160				

such as H-BN, ZnO, Al<sub>2</sub>O<sub>3</sub>, MgO, AlN, and SiC, have been used. These fillers have been used mainly for polymer composites to improve the thermal performance.<sup>6-13</sup>

Among the materials available, graphite has attracted significant attention owing to its remarkable properties, such as strong heat-resistance, electrical conductivity, low cost, light weight, high corrosion resistance, high dielectric constant, and high thermal conductivity.<sup>14-17</sup> Although graphite has an excellent thermal conductivity in the range of 200-800 W/mK, an inevitable drawback, i.e. the electrical conductivity, limits the applications of graphite/polymer composites.<sup>18</sup>

To overcome the aforementioned drawback, alumina, which has excellent electrical insulation, dielectric properties, high thermal conductivity, thermal stability, and corrosion resistance to a wide range of chemicals, is coated on the graphite surface. The electrical conductivity of the graphite can be reduced effectively by coating alumina on its surface. A range of techniques, such as chemical vapor deposition (CVD), physical vapor deposition (PVD), plasma sputtering, and sol-gel methods, have been used to coat alumina on the surface of graphite. The sol-gel method is one of the popular processes for synthesizing functional layers or particles because of its low-temperature processing and easy coating over a large surface compared to conventional film-formation techniques.<sup>18,19</sup>

This paper proposes a method to coat alumina on the graph-

ite under mild conditions that will endow graphite with electrically insulating properties. First, PVP@graphite was prepared in ethanol by physical adsorption, and a base-catalyzed sol-gel reaction of aluminum isopropoxide (AIP), the alumina precursor, was conducted in solution. PVP was used for the dense and uniform coating of alumina over the surface of the carbon substrates.<sup>20,21</sup> The alumina coated on the PVP@graphite improves the electrical resistivity of the synthesized alumina@PVP@graphite. With this background, the changes in morphology and the amounts of coated alumina, as well as the resulting electrically insulating properties were examined.

## Experimental

**Materials.** Two different sizes of synthetic graphite, KS6 (D<sub>90</sub> 6.5 μm) and KS44 (D<sub>90</sub> 45.4 μm), were supplied by Timcal (Switzerland). Aluminum isopropoxide (AIP, Al (OC<sub>3</sub>H<sub>7</sub>)<sub>3</sub>, ≥98%) from Sigma Aldrich (USA), ammonium hydroxide from OCI (S. Korea) and ethanol (extra pure grade) from Dusan Chemicals Co., Ltd. (S. Korea) were obtained. Epoxy resin and hardener were purchased from Kukdo Chemical Co. (S. Korea).

**Alumina Coating on the Surface of the Graphite.** The procedure for the alumina coating on the surface of the graph-

ite is as follows. The alumina@PVP@graphite was synthesized using a base-catalyzed sol-gel method, which is similar to the procedure reported elsewhere.<sup>20</sup> In our previous research, the coating reaction was performed in two steps: physical adsorption of PVP on the graphite surface and a silica coating on the PVP@graphite. In this study, the coating process was conducted with a different amount of PVP and AIP via a one-step reaction.

First, 2 g of raw graphite (KS6:KS44=1:1 w/w) powders were added to 100 mL of ethanol into which 3.2 g of PVP was dissolved. The solution was stirred mechanically for 4 h owing to the physical adsorption of PVP on the graphite surface. 0.8 g of NH<sub>4</sub>OH was then poured into the well dispersed solution and stirred for 30 min. 2.4 g of AIP was added to the solution and stirred vigorously for 24 h to coat alumina on the graphite surface.<sup>22</sup> After the coating process, the synthesized graphite was micro-filtered twice with ethanol to eliminate the solvents, residues, and byproducts.<sup>18</sup> The obtained product was kept in a vacuum oven at 70 °C overnight. The samples were then sintered at 600 °C for 2 h at a heating rate of 2 °C/min in N<sub>2</sub> gas in a furnace to improve the durability of the alumina layer on the graphite surface.<sup>23</sup> Fabrication of the other samples was conducted according to Tables 1 and 2.

**Characterizations.** To observe the morphology of the bulk, which is in layers and particles of alumina on the graphite surface, field emission transmission electron microscopy (FE-TEM, CM 2000, Philips) and scanning electron microscopy (SEM, Hitachi S-4300) were used. The quantitative change in the composition of the alumina@PVP@graphite was observed by thermogravimetric analysis (TGA, Diamond TG/DTA Lab System, Perkin Elmer Inc.) over the temperature range, 25-1000 °C, at a heating rate of 20 °C/min in air. Before TGA, the samples were dried overnight in a vacuum oven at 60 °C. An analysis of the synthesis of the filler focused on a role of PVP between the graphite and alumina, and a correlation between the alumina layer and the amounts of AIP. The changes in crystallinity and structures of the alumina@PVP@graphite were examined by recording the X-ray diffraction (XRD, D/MAX 200 V/PC, RIGAKU) patterns at a scan rate of 2 °/min in the Bragg angle ranging from 10° to 80° 2 $\theta$ . The surface resistivity was measured using two different devices: 1) a low resistivity meter (Loresta-GP, Mitsubishi Chemical Co., measurement range: 10<sup>-3</sup>-10<sup>7</sup>  $\Omega$ ) with a linear four-pin probe (ASP Probe), and 2) a high resistivity meter (Hiresta-UP, Mitsubishi Chemical Co., measurement range: 10<sup>4</sup>-10<sup>13</sup>  $\Omega$ ) connected to a concentric ring probe (URSS Probe). The surface area ( $S_{\text{BET}}$ )

of the alumina@PVP@graphite was obtained using the Brunauer-Emmett-Teller (BET) method with a volumetric adsorption analyzer (ASAP ZOZO, Micromeritics Co.).

## Results and Discussion

Experiments were conducted to obtain the optimal alumina coating on the graphite surface with or without PVP. SEM and FE-TEM were used to examine the changes in the morphology and coverage of the alumina@PVP@graphite with two different variables; the amounts of AIP and PVP. Figure 1(a)-(c) and (g)-(i) display the surface of the composite materials from 0 to 80 wt% AIP. The primary alumina particles are generated on the surface of the graphite, and they grow into the layers. At 80 to 120 wt% AIP, the layers were connected and combined together, as shown in Figure 1(d)-(e) and (j)-(k). At 160 wt% AIP, an excess of AIP formed protruding bulks of alumina on the existing alumina layer based on their high affinity (Figure 1(f) and (l)). The result for 120 wt% AIP to the graphite showed the best morphology, which is well coated without outgrowths and superfluity. The images in Figure 1 show the growth of alumina layers and particles on PVP@graphite according to the increase in AIP. This means that as more of the alumina precursor is activated in the sol-gel reaction, more alumina layers and particles form on the graphite surface.

In Figure 2(a) and (f) for 0 wt% PVP, many alumina particles were attached roughly to the alumina layer on graphite. In Figure 2(b)-(d) and (g)-(i), which display the surface from 20 to 80 wt% PVP, the layers of alumina were smooth, which combined the layer with the particles according to the increase in PVP. In Figure 2(e) and (j) for 160 wt%, there are no roughly protruding alumina particles. A uniform layer of alumina on the PVP@graphite was well formed. The result for 160 wt% PVP to graphite showed the best morphology. Figure 2 shows a uniform or rough form of the alumina layers and particles on the PVP@graphite according to increase in PVP. PVP on the graphite helped form a uniform layer of alumina on PVP@graphite and decrease the amounts of surplus particles and bulks of alumina. Therefore, an increase in the PVP content results in 1) improvement in the uniform surface coating of alumina on the PVP@graphite and 2) decrease in the size and amounts of alumina particles and bulks of the outside of the layer.

Figure 3 shows overall mechanism of the coating process and the role of PVP in the formation of the layer of alumina. The importance of PVP is shown in Figure 3(a) and (b).

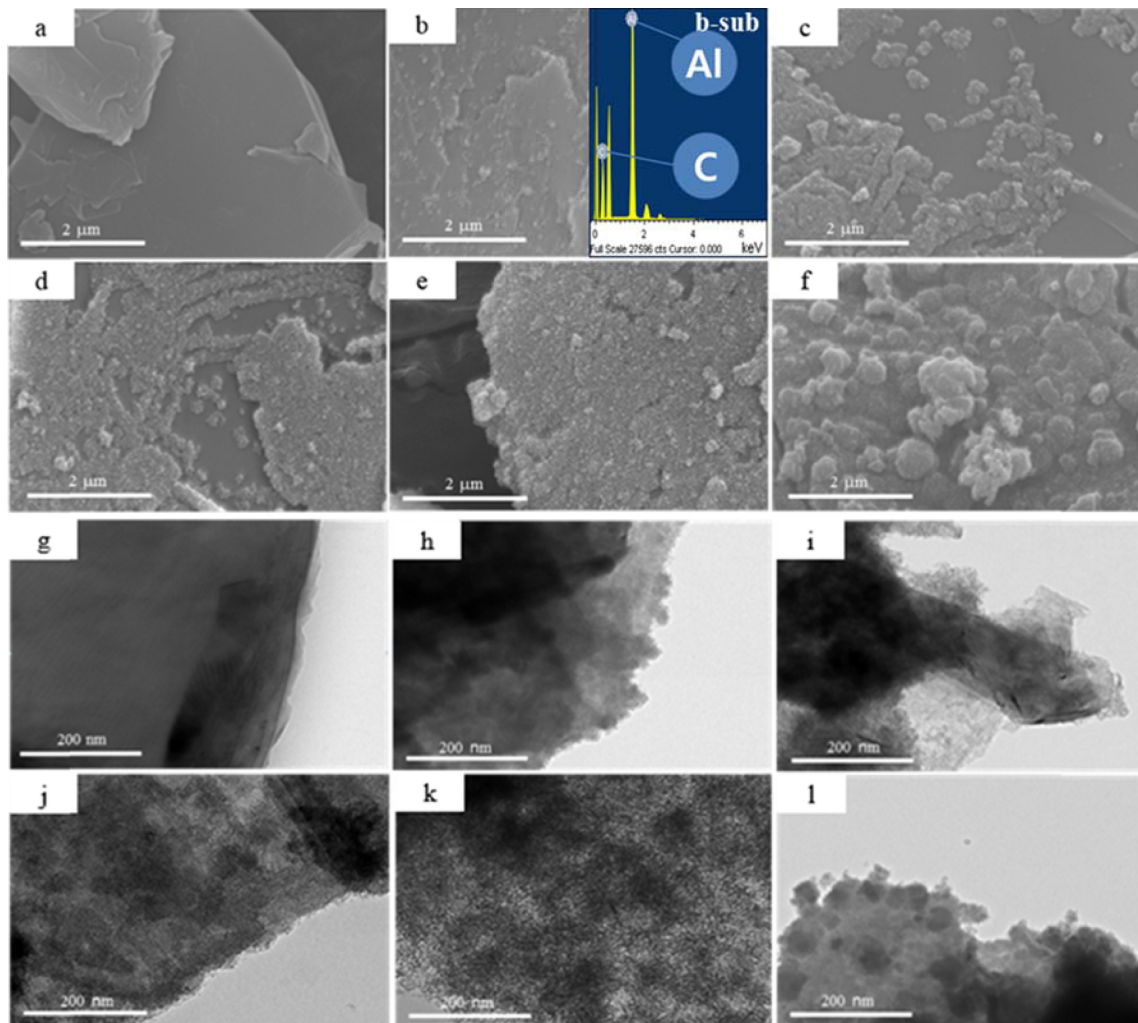


**Figure 1.** Scanning electron microscopy images of alumina@PVP@graphite with different amounts of AIP (a) 0; (b) 20; (c) 40; (d) 80; (e) 120; (f) 160%; field emission transmission electron microscopy of alumina@PVP@graphite with different amounts of AIP (g) 0; (h) 20; (i) 40; (j) 80; (k) 120; (l) 160%.

During the coating process, the alumina particles were synthesized in basic atmosphere media via a sol-gel reaction, and underwent a condensation reaction and size growth. Without PVP, the alumina particles are unable to generate a uniform layer of alumina on the graphite surface and many alumina particles with diverse sizes in the alcoholic medium were formed because alumina and its precursor have poor chemical affinity to the hydrophobic surface of graphite. This concept is displayed in Figure 3(a). In contrast, Figure 3(b) shows that alumina particles with a uniform size were produced and they formed layers of smooth shapes because of the hydrogen bonds between PVP and AIP. Figure 3 shows the interaction between the ketone groups of PVP and hydroxyl groups derived from AIP. Initially, AIP is changed to aluminum

hydroxide by a hydrolysis reaction with water from ethanol, as shown in Figure 3(c). This reaction was catalyzed by ammonium hydroxide. The hydrogen atoms in aluminum hydroxide combine with PVP to provide oxygen and nitrogen through hydrogen bonds. The nitrogen and oxygen atoms of PVP behave as active sites, which can make a hydrogen bond with the hydroxyl groups and result in the uniform coverage of alumina layers over the graphite surface in the presence of PVP.

Figure 4(a) shows the TGA curves of the alumina@PVP@graphite according to the amounts of AIP input. The initial temperature for the thermal degradation of raw graphite is approximately 700 °C. Alumina@PVP@graphite presents two-step degradation in the TGA curves overall. The weight loss of alumina@PVP@graphite corresponds to non-reacted

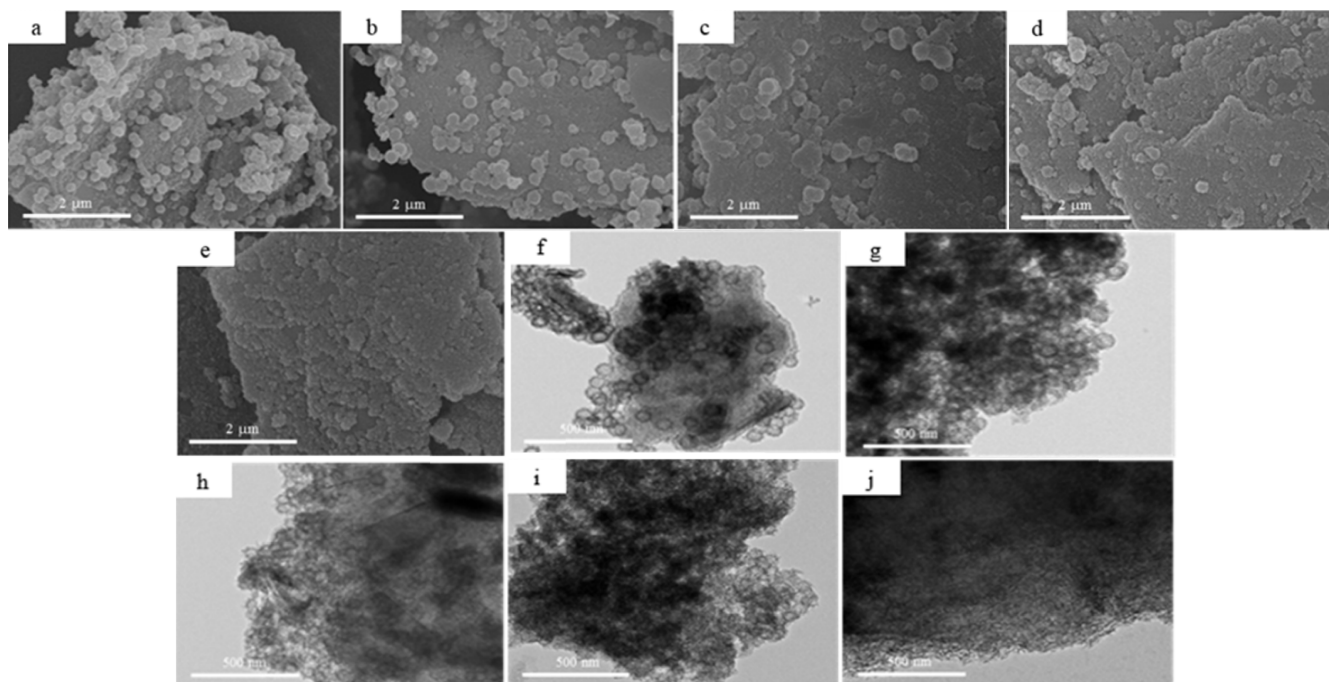


**Figure 2.** Scanning electron microscopy images of (a) alumina-coated graphite without PVP, and alumina-coated graphite with various mass percentages of PVP (b) 20; (c) 40; (d) 80; (e) 160%; field emission transmission electron microscopy images of (f) alumina-coated graphite without PVP, and alumina-coated graphite with various mass percents of PVP (g) 20; (h) 40; (i) 80; (j) 160%.

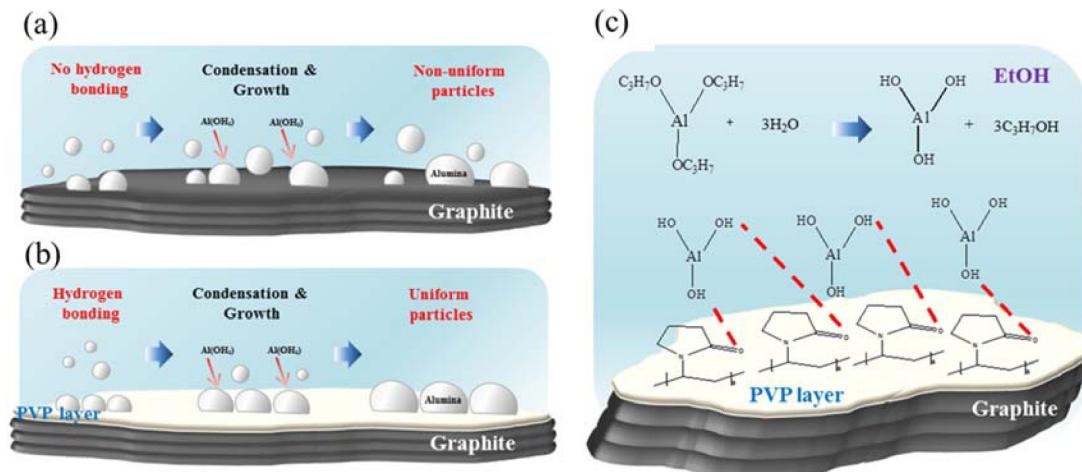


**Figure 3.** (a) Coating alumina on the graphite without PVP; (b) with PVP; (c) coating mechanism of alumina@PVP@graphite.

alumina precursors, which are decomposed up to 700 °C. In the TGA curve of the alumina@PVP@graphite using 160 wt% AIP to graphite, more non-reacted precursors undergo decomposition than others. In particular, this behavior is observed in the first degradation. In the second degradation, the thermal residues mean the amounts of alumina in alumina@PVP@graphite that are generated via the coating process. The results show a correlation between the amounts of AIP and the

thermal residues, which concurs with SEM and TEM. Figure 4(b) shows the TGA curves of the raw graphite, alumina@graphite, and alumina@PVP@graphite. Compared to the two-step degradation of alumina@graphite and alumina@PVP@graphite, raw graphite degrades in a single step. This is based on the mass loss of non-reacted alumina precursors, which are decomposed by oxygen in the first degradation step. At temperatures over 700 °C, the curve for the

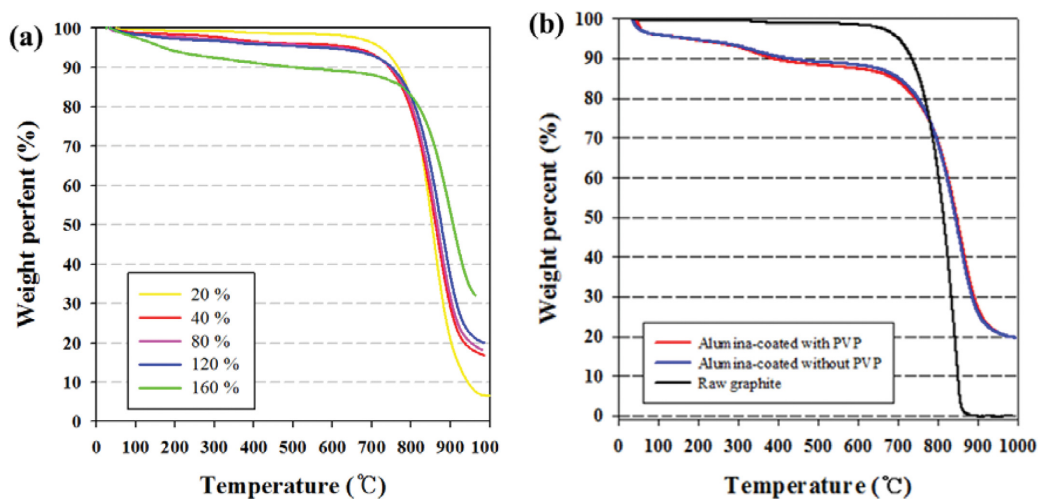


**Figure 4.** Thermogravimetric analysis of (a) alumina@PVP@graphite according to the AIP content; (b) comparisons of raw graphite, alumina@graphite and alumina@PVP@graphite.

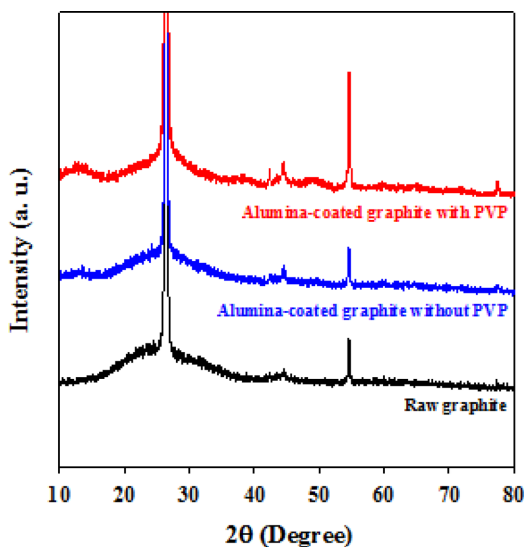


**Figure 5.** X-ray diffractions of raw graphite, alumina@graphite, and alumina@PVP@graphite.

weight percent of raw graphite goes to zero, whereas those of alumina@graphite and alumina@PVP@graphite decrease from approximately 88% to 20%. The shape of the curve for weight loss of the alumina@graphite resembles that of the alumina@PVP@graphite, which means that there is no significant difference in the decomposition temperature and mass loss. This suggests that the existence of PVP on the graphite surface does not influence the amounts of coated alumina.

Figure 5 presents XRD patterns of the samples after thermal sintering in nitrogen gas at 600 °C. The peaks for the graphite did not change even after the sol-gel reaction in the basic

medium, which means that the crystalline structures of graphite are not destroyed. The XRD pattern showed a broad peak for amorphous alumina-coated graphite between 11° and 17°. A peak between 45° and 47° was assigned to gamma alumina, which has a crystallite size of 5–10 nm after thermal sintering of 600 °C.<sup>24</sup>

Figure 6(a) and (b) show the surface resistivity of the samples. According to these results, the coverage of the alumina layer on the graphite surface is influenced by the amounts of supplied AIP and use of PVP. The surface coverage has a close relationship with the surface resistivity. Figure 6(a) shows that the surface resistivity of the alumina@PVP@graphite increases from  $10^4$  to  $10^{12}$  ohm/sq in the precursor content ranging from 20 to 120%. This means that AIP is provided mainly by forming the alumina layer, which endows the graphite with insulating properties in the range of contents. In contrast, there was no substantial increase in the surface resistivity at precursor contents ranging from 120 to 160 wt%. In the range of the precursor contents, the amount of the AIP forms unnecessary alumina bulk according to SEM and TEM. Therefore, 120 wt% AIP is the optimal amount. Figure 6(b) shows that the surface resistivity of the alumina@PVP@graphite and alumina@graphite improved from  $2.3 \times 10^2$  to  $2.7 \times 10^{12}$  ohm/sq and to  $1.3 \times 10^{10}$  ohm/sq, respectively. These values show the roles of the alumina layer, especially, PVP. The alumina@PVP@graphite is categorized as an electrical insulator, but alumina@graphite is not. The use of PVP to produce a homogeneous and uniform alumina coating clearly affects the electrical resistivity of the final sample.

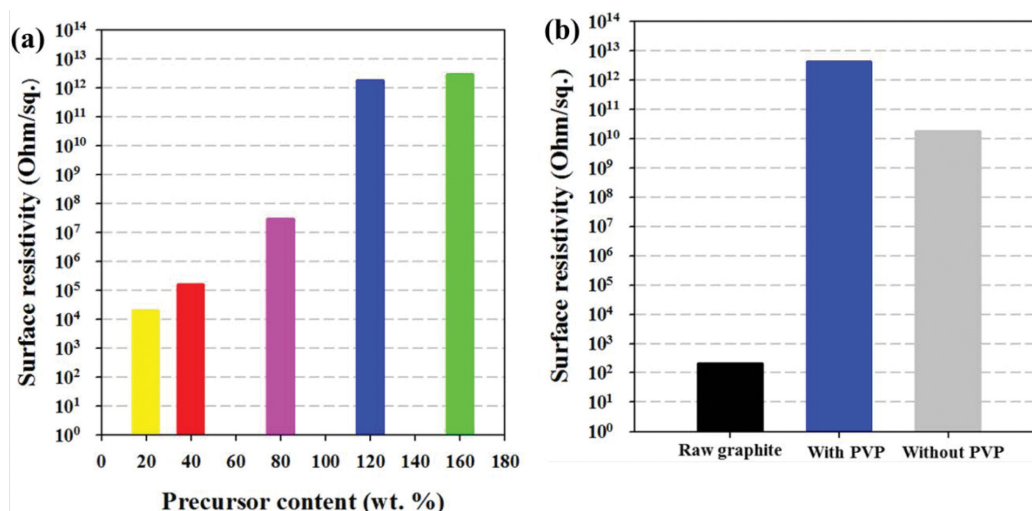


**Figure 6.** Surface resistivities of (a) alumina@PVP@graphite according to AIP content; (b) comparisons of that of raw graphite, alumina@graphite, and alumina@PVP@graphite.

**Table 3. Surface Area of Raw Graphite, Alumina@Graphite and Alumina@PVP@Graphite**

No.	Sample	Surface area ( $\text{m}^2/\text{g}$ )
1	Raw graphite	14.42
2	Alumina-coated graphite without PVP	123.84
3	Alumina-coated graphite with PVP	101.96

The surface area of raw graphite, alumina@graphite and alumina@PVP@graphite were 14.42, 123.84, and 101.96  $\text{m}^2/\text{g}$ , respectively (Table 3). Raw graphite showed the lowest surface area. The layers of alumina provide alumina@PVP@graphite and alumina@graphite with 7-9 times larger surface area than raw graphite. The surface area of alumina@graphite increased by approximately 21% compared to those of the alumina@PVP@graphite. The rough morphology involving the excess bulk and particles on the alumina@graphite surface has a larger surface area than that of the uniform and smooth shapes of the alumina@PVP@graphite, as observed by SEM and FE-TEM.

## Conclusions

PVP@graphite was coated with a uniform alumina layer by a sol-gel reaction in basic medium. Analysis of the synthesis of the filler focused on the role of PVP between the graphite and alumina, and the correlation between the alumina layer and the amounts of AIP. The effects of the amounts of alumina pre-

cursor and cohesion promotor on the surface morphology and surface resistivity of alumina@PVP@graphite and alumina@graphite were examined. The following conclusions could be drawn.

1) PVP on the graphite plays a critical role in coating the graphite with a uniform alumina layer. According to the increase in PVP, the layers of alumina become smooth and the quantity of surplus alumina particles and bulk are reduced.

2) Alumina layer provides alumina@PVP@graphite and alumina@graphite with a surface resistivity of approximately  $10^{12}$  and  $10^{10}$  ohm/sq. The synthesized alumina@PVP@graphite can be categorized as an electrical insulator with a high surface resistivity of approximately  $10^{12}$  ohm/sq.

**Acknowledgment:** This study was supported by Regional Innovation Center for Environmental Technology of Thermal Plasma (ETTP) at INHA University designated by MOCIE (grant no.: 1415139264).

## References

1. W. ThongRung, R. J. Spontak, and C. M. Balik, *Polymer*, **43**, 2279 (2002).
2. P. K. Schelling, L. Shi, and K. E. Goodson, *Mater. Today*, **8**, 30 (2005).
3. D. G. Cahill, W. K. Ford, K. E. Goodson, G. D. Mahan, A. Majumdar, H. J. Maris, R. Merilin, and S. R. Phillpot, *J. Appl. Phys.*, **93**, 793 (2003).
4. L. Shi, D. Li, C. Yu, W. Jang, W. Kim, D. Kim, Z. Yao, P. Kim, and A. Majumdar, *J. Heat Trans-T ASME*, **125**, 881 (2003).

5. M. Liu, W. Saman, and F. Bruno, *Renew. Sust. Energ. Rev.*, **16**, 2118 (2012).
6. A. Yu, P. Ramesh, M. E. Itkis, E. Bekyarova, and R. C. Haddon, *J. Phys. Chem. Lett.*, **111**, 7565 (2007).
7. S. Ganguli, A. K. Roy, and D. P. Anderson, *Carbon*, **46**, 806 (2008).
8. M. B. Bryning, D. E. Milkie, M. F. Islam, J. M. Kikkawa, and A. G. Yodh, *Appl. Phys. Lett.*, **87**, 161909 (2005).
9. A. Moysala, Q. Li, I. A. Kinloch, and A. H. Windle, *Compos. Sci. Technol.*, **66**, 1285 (2006).
10. K. C. Yung and H. Liem, *J. Appl. Polym. Sci.*, **106**, 3587 (2007).
11. J.-U. Ha, J. Hong, M. Kim, J. K. Choi, D. W. Park, and S. E. Shim, *Polym. Korea*, **37**, 722 (2013).
12. Y. P. Mamunya, V. V. Davydenko, P. Pissis, and E. V. Lebedev, *Eur. Polym. J.*, **38**, 1887 (2002).
13. Y. Kim, S. H. Baek, and S. E. Shim, *Polym. Korea*, **38**, 378 (2014).
14. M. L. Guzman-Castillo, X. Bokhimi, A. Toledo-Antonio, J. Salmenes-Blasquez, and F. Hernandez-Beltran, *J. Phys. Chem. B*, **105**, 2099 (2001).
15. L. Fu, Y. Liu, Z. Liu, B. Han, L. Cao, D. Wei, G. Yu, and D. Zhu, *Adv. Mater.*, **18**, 181 (2006).
16. K. Kawabata, H. Yoshimatsu, E. Fujii, K. Hiragushi, A. Osaka, and Y. Miura, *J. Mater. Sci. Lett.*, **20**, 851 (2001).
17. S. Choi, K. Kim, J. Nam, and S. E. Shim, *Carbon*, **60**, 254 (2013).
18. T. D. Dao, H. Lee, and H. M. Jeong, *J. Colloid Inter. Sci.*, **416**, 38 (2014).
19. Q. Zeng, *J. Appl. Polym. Sci.*, **70**, 177 (1998).
20. S. Choi, Y. Kim, J. H. Yun, I. Kim, and S. E. Shim, *Mater. Lett.*, **90**, 87 (2013).
21. M. Pattanaik and S. K. Bhaumik, *Mater. Lett.*, **44**, 352 (2000).
22. S. Yilmaz, Y. Kutmen-Kalpakli, and E. Yilmaz, *Ceram. Int.*, **35**, 2029 (2004).
23. S. Zhang and W. E. Lee, *J. Eur. Ceram. Soc.*, **23**, 1215 (2003).
24. S. Cava, S. M. Tebcherani, I. A. Souza, S. A. Poanaro, C. A. Paskocimas, E. Longo, and J. A. Varela, *Mater. Chem. Phys.*, **103**, 394 (2007).